

Porous metal–organic frameworks (MOFs) as matrices for inclusion compounds

Kinetic stability under heating

V. A. Logvinenko · M. P. Yutkin · M. S. Zavakhina · V. P. Fedin

Bretsznajder Special Chapter
© Akadémiai Kiadó, Budapest, Hungary 2012

Abstract Inclusion compounds based on metal–organic frameworks (MOFs) have promising practical application in gas storage, separation and fine purification of substances, as well as in catalysis. MOFs are crystalline compounds consisting of metal ions coordinated by bridging organic ligands that form porous structures. The kinetics of the thermal decomposition of the frameworks themselves, namely [Co₂(camph)₂bpy] and [Co₂(asp)₂bpy], was investigated (camph and asp are the anions of camphoric and aspartic acids, bpy is the organic amine, 4,4'-bipyridyl). The empty coordination polymer framework based on metal camphorates was thermally (kinetically) less stable than the polymer framework based on metal aspartate. A high kinetic stability of frameworks with aspartic complexes during heating was due to the entropic factor rather than the enthalpic one.

Keywords Coordination compounds · Inclusion compounds · Kinetic stability · Non-isothermal kinetics

Introduction

This article explored the stability of the important part of supramolecular compounds: inclusion compounds, based on coordination compounds as host matrices.

Many different inclusion compounds are currently known. As a rule, the processes of removing guest

molecules are studied by thermal analysis methods, that is, the stability of inclusion compounds under heating. Cyclodextrin-based inclusion compounds are a good example of such thorough investigations [1–3].

Metal–organic coordination polymer frameworks (MOFs) are a relatively new matrix type; their “empty” structures can remain after guest molecule removal. MOFs are crystalline compounds consisting of metal ions coordinated by bridging organic ligands, which form one-, two- or three-dimensional structures that can be porous. Tremendous interest in these compounds is due to their promising practical application, first of all, for gas storage (such as hydrogen, methane, acetylene, and carbon dioxide), separation and fine purification of substances, and also catalysis. The possibility of a wide functional design of these structures is essential: variation of the length of bridging organic ligands can change cavity sizes and the obtained coordination framework can maintain the porous structure for an infinitely long time [4, 5]. Quantitative data on the thermodynamic and kinetic stability of inclusion compounds and porous frameworks themselves are very important for estimating their general stability.

Experimental

Studied compounds [4, 5]

A series of metal–organic coordination polymers were obtained by varying transition metal cations, optically pure ligands and bridging ligands (linkers). Salts of divalent zinc, copper, and cobalt were used as the source of cations.

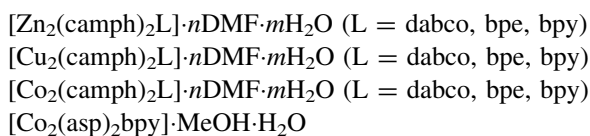
In this study, we used optically pure: *R,S*-camphoric acid (*R,S*-H₂camph), and *S*-aspartic acid (*S*-H₂asp). Diazabicyclo[2.2.2]octane (dabco), 4,4'-bipyridyl (bpy), and

V. A. Logvinenko (✉) · M. P. Yutkin · M. S. Zavakhina · V. P. Fedin
Nikolaev Institute of Inorganic Chemistry, Siberian Branch of the Russian Academy of Sciences, Ac. Lavrentiev Ave. 3, Novosibirsk-90, Russia 630090
e-mail: val@niic.nsc.ru

trans-bis(4-pyridyl)ethylene (bpe) were employed as the source of rigid bridging ligands (Fig. 1).

The synthesis was carried out in solutions with thermostating at a temperature below the boiling point of the solvent (H₂O, DMF, CH₃OH or their mixtures). The structure of most of the obtained compounds was determined by single crystal XRD.

Studied compounds:



M = Zn, Cu, Co; H₂L are dibasic acids; L is the camphorate anion (C₁₀H₁₄O₄²⁻) or the aspartic anion (C₄H₅NO₄²⁻); the linkers are organic amines: dabco, bpy, and bpe (Fig. 1).

Thermal analysis

TG measurements were carried out on a Netzsch thermal analyzer TG 209 F1. The experiments were performed in the argon flow (70 cm³ min⁻¹) at heating rates of 5, 10, and 20 K min⁻¹; the sample weight was kept cca 5.0 mg or cca 15 mg. Thermomechanical analysis (dilatometry) was carried out on a Netzsch thermal analyzer TMA 202; the powder layer thickness was 1.02–1.03 mm (with a sample weight of 42–45 mg).

Kinetic analysis under non-isothermal conditions

Thermogravimetric data were processed with the computer program Netzsch Thermokinetics 2 (Version 2004.05) [6]. A special program module “Model-free”, based on the well-known studies [7–16], allows one to process several thermogravimetric curves obtained with different heating rates and calculate the activation energy without preliminary information about kinetic topochemical equations. The Friedman method was used to calculate the activation energies for each experimental point of fractional

conversion (in the range 0.005 < α < 0.995). We further used the same set of experimental data to search for the topochemical equation (the selection was made from 16 equations: chemical reaction at the interface, nucleation, and diffusion). This calculation is made by the improved differential procedure of Borchardt–Daniels within the multiple linear regression approach [6]. It is very important that the range of the degree of conversion (α) for this calculation is chosen based on the relative constancy of the calculated kinetic parameters from the Friedman analysis. The *F* test was used to search for the best kinetic description.

The *F* test was used for the statistical control of the obtained equation. It tests the residual variance of individual models against one another and answers the question of whether the models differ significantly (statistically) or not. If $F_{\text{exp}(1)} \approx F_{\text{exp}(2)}$ for two equations, there is no reason to assume the first model is better for characterizing the experiment. The statistical quantile F_{crit} is obtained for a level of significance of 0.05.

If the calculation results in two or three kinetic equations with close values of the correlation coefficients and the *F* test, but with noticeably different values of kinetics parameters, it is more correct to choose the equation with activation energy values close to the data of the “Model-free” module program. Discrimination between the two steps is very relative in this search for topochemical equations, but it helps to find the most reliable ones. The special program of nonlinear regression is useful in searching for a full set of kinetic parameters for multistep processes. The closest fit between the activation energies from the “Model-free” analysis and the nonlinear regression calculation is an important from a physicochemical point of view. Therefore, the authors of the computer program used recommend to fix E_a values (obtained by linear regression and congruent with E_a from the “Model-free” analysis) in the calculations with this program.

The random error in the activation energy values for such a reversible decomposition reaction is usually about 10% in these experiments, which we took into consideration. The computer program Netzsch Thermokinetics 2 enables the estimation of the contribution of the steps (in Δm percentage) after this nonlinear regression calculation.

The well-known recommendations for performing kinetic computations on thermal analysis data [17] were used.

There are several important assumptions and limitations. The kinetic equations used for the calculation of the kinetic parameters are topochemical and the calculated parameters (E and A) are formal and conventional from the standpoint of the classical chemistry of solids.

The course (general trend) in the variation of these values within a selected series of compounds is very

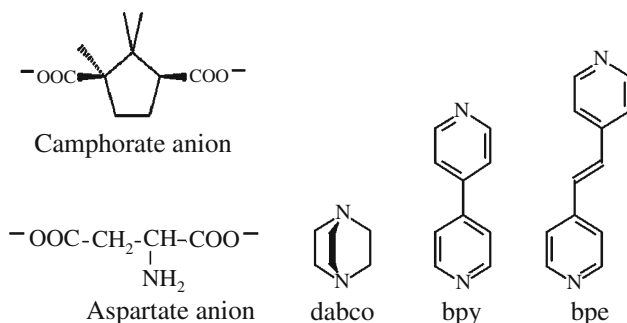


Fig. 1 Used ligands (acid anions and linkers)

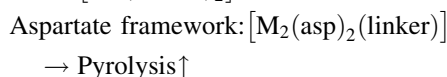
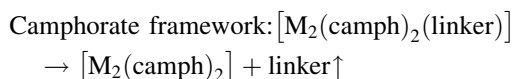
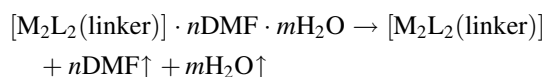
important: either isostructural or genetically related compounds. The best series are [18–20]:

- (1) Coordination compounds with volatile ligands (water, amines with one central atom and different ligands or with different central atoms and the same ligand).
- (2) Inclusion compounds with one host matrix and different guest molecules or with different host matrices and the same guest molecule.

The studied compounds belonged to this list.

Results and discussion

The studied thermal decomposition reactions were:



The camphorate framework and the aspartate framework have different structures [4, 5].

There were channels in the frameworks: $3 \times 4 \text{ \AA}$ for $[M_2(\text{camph})_2\text{dabco}]$ derived compounds, $5 \times 7 \text{ \AA}$ for $[M_2(\text{camph})_2\text{bpy}]$ derived compounds and $5 \times 10 \text{ \AA}$ for $[M_2(\text{camph})_2\text{bpy}]$ derived compounds. There were binuclear fragments $[\text{Co}_2(\text{COOR})_4]$ with the Chinese lantern structure in the camphorate compounds. These fragments were combined together by camphorate bridges into two-dimensional layers. These infinite plane layers did not include nitrogen donor atoms from linker ligands. When these infinite layers were combined with linker ligands (by means of nitrogen atoms), the coordination number of the Co cation increased from 4 to 6, and the bulk framework structure was created.

The coordination octahedron in the aspartate compounds contained two nitrogen atoms (from the aspartic amino group and the linker ligand) and four oxygen atoms from the carboxylic groups of two aspartic ions. Hence, the aspartic anion was a tridentate ligand coordinated to the cobalt cation by one amino group and carboxylic groups. There were no independent two-dimensional layers; the whole bulk framework was simultaneously built from the aspartic anions and linker ligands.

Decomposition of $[\text{Zn}_2(\text{camph})_2\text{bpe}] \cdot n\text{DMF} \cdot m\text{H}_2\text{O}$ inclusion compound [21]

The $[\text{Zn}_2(\text{camph})_2\text{bpe}] \cdot 5\text{DMF} \cdot \text{H}_2\text{O}$ inclusion compound lost both water and dimethylformamide (DMF) molecules under heating; the next step of the decomposition was the loss of the

N-donor ligand (linker) ($\approx 510 \text{ K}$). Mass loss was a multi-step process, which was confirmed by the DTG curves; and we attributed the very first small (and confirmed by DTG) step of mass loss to water removal (cca 1.7% mass).

The inclusion compound was destructed into an X-ray-amorphous matrix substance and not restored to the initial state after interaction with DMF [4, 5]. The “empty” matrix structure (more than half-empty, with 55% of the porous part) was not stable at all (thermodynamically and kinetically), whereas the “filled” matrix structure could only be synthesized when it assembled during the synthesis: $\{\text{Zn}(\text{NO}_3)_2 \cdot 6\text{H}_2\text{O} + \text{H}_2\text{camph} + \text{DMF} + \text{bpe}\}$. This means that the expanded matrix of the $[\text{Zn}_2(\text{camph})_2\text{bpe}] \cdot 5\text{DMF} \cdot \text{H}_2\text{O}$ coordination compound can be synthesized only with support of the guest by assembling around DMF molecules [21]. Such a structure must have low stability. Thermomechanical analysis showed that the “empty” structure of $[\text{Zn}_2(\text{camph})_2\text{bpe}]$ (55% porous) was not stable at all; therefore, the sample volume decreased considerably and steadily during DMF removal (330–500 K). The next decrease in the sample volume (510–560 K) was due to bpe removal [21].

The aspartate framework was somewhat more stable than the camphorate one (Fig. 2).

Decomposition of the $[\text{Co}_2(\text{camph})_2\text{bpy}]$ matrix compound: $[\text{Co}_2(\text{camph})_2\text{bpy}] \rightarrow [\text{Co}_2(\text{camph})_2] + \text{bpy}\uparrow$.

The decomposition of the $[\text{Co}_2(\text{Camph})_2(\text{bpy})]$ empty framework began at 570 K (Fig. 3); the first part of the decomposition corresponded to the removal of the bpy ligand. The kinetics of this process was studied.

“Model-free” data are presented in Fig. 4. The activation energy can be considered as constant for the Friedman method: $E = 257 \pm 10 \text{ kJ/mol}$ ($5\% < \alpha < 90\%$).

Equations An, Fn were indistinguishable by the *F* test (Table 1).

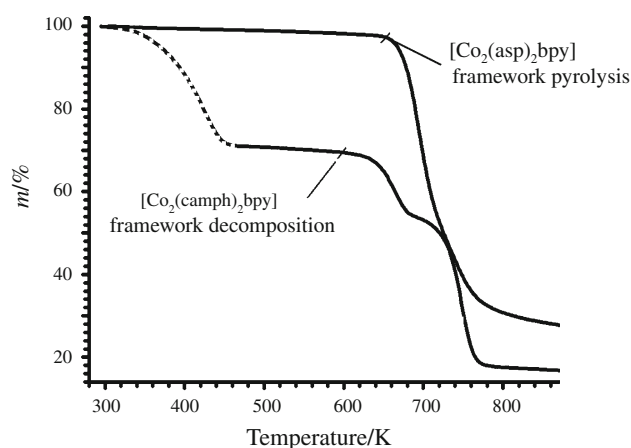


Fig. 2 TG curves for the decomposition of $[\text{Co}_2(\text{camph})_2\text{bpy}] \cdot 3\text{DMF}$ and $[\text{Co}_2(\text{Asp})_2\text{bpy}]$; $m \approx 5 \text{ mg}$; argon flow $70 \text{ cm}^3 \text{ min}^{-1}$; heating rate 20 K min^{-1}

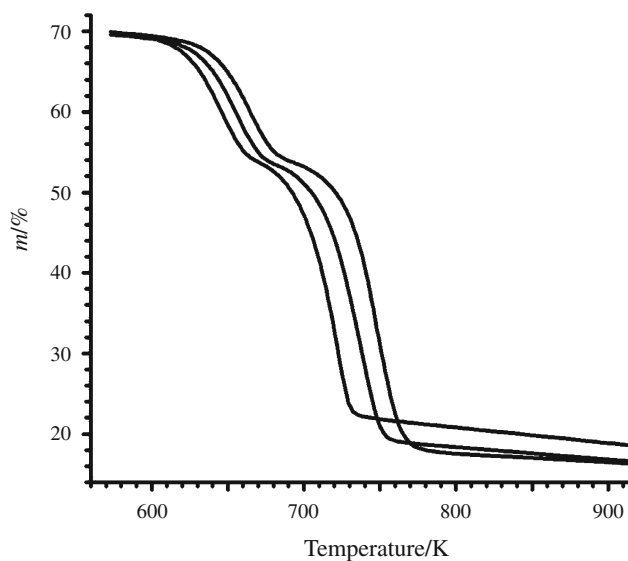


Fig. 3 TG curves for the decomposition of the $[\text{Co}_2(\text{camph})_2\text{bpy}]$ framework, $m \approx 5.0$ mg; argon flow $70 \text{ cm}^3 \text{ min}^{-1}$; heating rates 5, 10, and 20 K min^{-1}

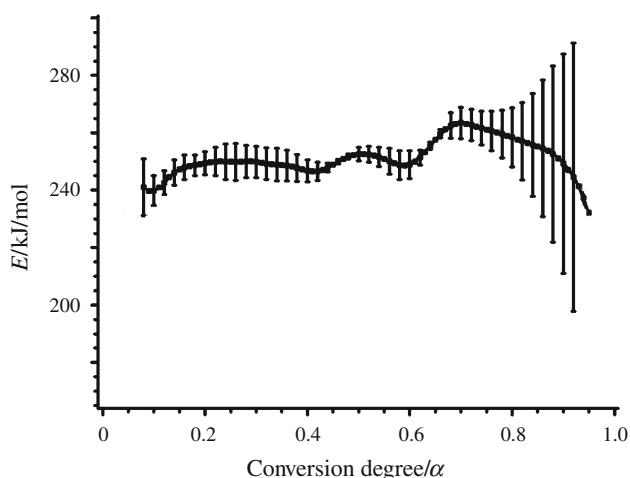


Fig. 4 Friedman analysis of the decomposition of the $[\text{Co}_2(\text{camph})_2\text{bpy}]$ framework: activation energies depending on the degree of conversion

Table 1 Decomposition of $[\text{Co}_2(\text{camph})_2\text{bpy}]$

F_{exp}	F_{crit}	f-act	Equation	$E/\text{kJ mol}^{-1}$	$\lg A$
1.00	1.11	1040	An	253 ± 1	18.2 ± 0.1
1.94	1.11	1040	Fn	234 ± 2	16.7 ± 0.2
7.60	1.11	1040	D3		

Data of the F test of fit quality/to search for the best kinetic description, $\alpha = 0.005\text{--}0.995$

$$\text{An, } f(\alpha) = (1 - \alpha)/[-\ln(1 - \alpha)]^{0.15};$$

$$\text{Fn, } f(\alpha) = (1 - \alpha)^{1.01}.$$

Fn equation corresponded to the nucleation process. The correlation coefficient was 0.998818 (Fig. 5).

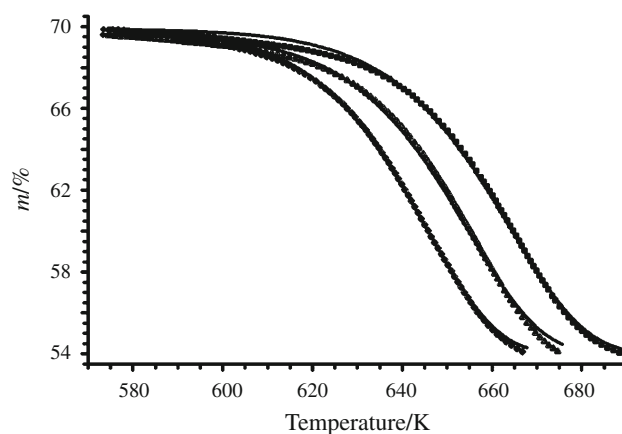


Fig. 5 Decomposition of the $[\text{Co}_2(\text{camph})_2\text{bpy}]$ framework. Data processing: non-linear regression curve fitting simulated with the equation Fn. The range of the degree of conversion for the calculation: $0.005 \leq \alpha \leq 0.995$. Experimental points, calculated lines

Decomposition of $[\text{Co}_2(\text{asp})_2\text{bpy}]$ matrix compounds:
 $[\text{Co}_2(\text{asp})_2\text{bpy}] \rightarrow (\text{Pyrolysis}) \rightarrow$

The $[\text{Co}_2(\text{asp})_2\text{bpy}]$ framework was stable until ≈ 600 K. The decomposition of the $[\text{Co}_2(\text{asp})_2\text{bpy}]$ framework had two stages (Fig. 6); we studied the decomposition kinetics for the first stage.

“Model-free” data are given in Fig. 7. The activation energy can be considered as variable in compliance with the Friedman method.

We calculated the kinetic parameters for the two-step process (Table 2).

The best description for the two-step process ($A \rightarrow B \rightarrow C$) is: the first step: An, the second step: Fn (Fig. 8): $f_1(\alpha) = (1 - \alpha)/[-\ln(1 - \alpha)]^{0.36}$; $f_2(\alpha) = (1 - \alpha)^{0.54}$.

The correlation coefficient was 0.997220. We estimated the contribution of the steps: the first step was 1% and the second step 99% of the decomposition.

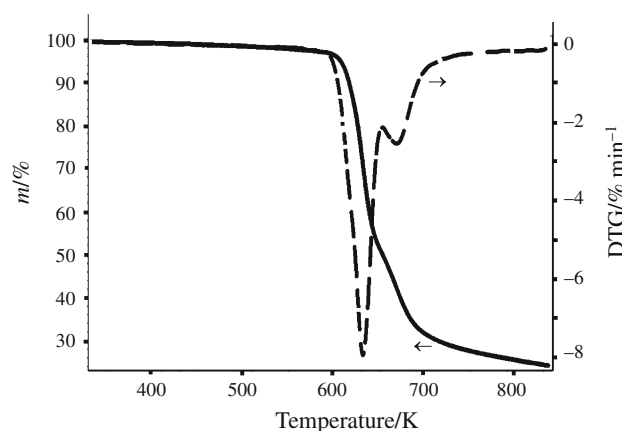


Fig. 6 TG and DTG curves of the decomposition of the $[\text{Co}_2(\text{Asp})_2\text{bpy}]$ framework; $m \approx 5.0$ mg; argon flow $70 \text{ cm}^3 \text{ min}^{-1}$; heating rate 10 K min^{-1}

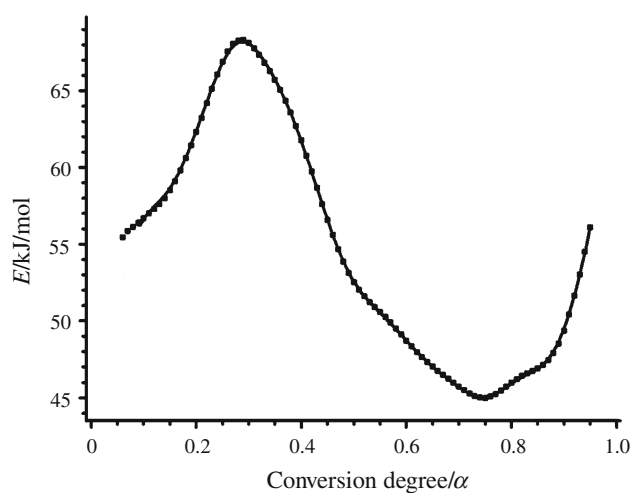


Fig. 7 Friedman analysis of $[\text{Co}_2(\text{asp})_2\text{bpy}]$ decomposition: activation energies depending on the degree of conversion

Table 2 Decomposition of $[\text{Co}_2(\text{asp})_2\text{bpy}]$

F_{exp}	F_{crit}	f-act	Equation	$E/\text{kJ mol}^{-1}$	lgA
1.00	1.12	875	I. An	60.0 ± 0.1	2.6 ± 0.1
			II. Fn	62.8 ± 0.2	1.8 ± 0.1
19.44	1.12	882	An	73 ± 1	3.2 ± 0.1
33.84	1.12	883	B1		
46.98	1.12	882	Fn		

Data of the F test of fit quality/to search for the best kinetic description, $\alpha = 0.005\text{--}0.995$

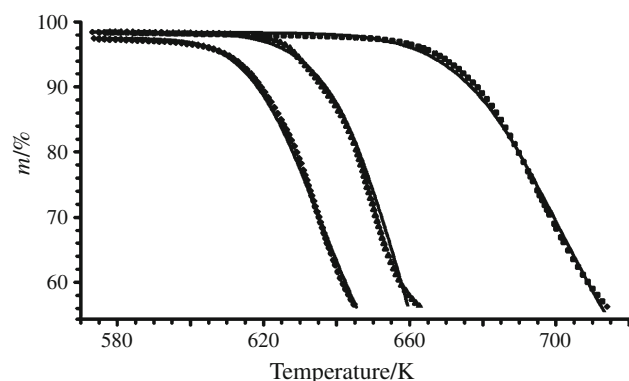


Fig. 8 $[\text{Co}_2(\text{asp})_2\text{bpy}]$ decomposition. Data processing: non-linear regression curve fitting simulated with the equation An. The range of the degree of conversion for the calculation: $0.005 \leq \alpha \leq 0.995$. Experimental points, calculated lines

Therefore, the results for the kinetic stability of the $[\text{Co}_2(\text{asp})_2\text{bpy}]$ framework were: $E = 60\text{--}63$ kJ/mol, $\log A = 1.8\text{--}2.6$.

The aspartate framework was somewhat more stable than the camphorate one (Fig. 2), but the activation energy of the decomposition of the $[\text{Co}_2\text{Camph})_2\text{bpy}]$ framework

was considerably higher than that of the decomposition of the $[\text{Co}_2(\text{Asp})_2\text{bpy}]$ framework ($E_1 = 234$ kJ/mol and $E_2 = 63$ kJ/mol); however, the pre-exponential factor was substantially smaller in the second case ($\log A_1 = 16.7$ and $\log A_2 = 1.8$).

This contribution decreased the decomposition rate constant of the framework with the aspartic ligand.

The loss of linker molecules in the framework with the aspartic complex did not occur because of steric hindrances. The pyrolysis of organic ligands started at ≈ 600 K.

An empty framework of the coordination polymer with metal camphorates was sterically unstable and decomposed with the release of the organic amine (linker). Therefore, high kinetic stability of the framework with aspartic complexes during heating was due to the entropic factor rather than the enthalpic one.

Conclusions

Empty structures of camphorate–ion based coordination polymers with large channels (5×7 and 5×10 Å) are unstable after the removal of guest molecules and they easily lose bpy and bpe ligand linkers at low temperatures [21].

After removal of guest molecules, the structure of the coordination polymer based on the aspartic ion is stable to the loss of the linker ligand because the donor nitrogen atom of the linker is involved in an infinite layer of the framework. The destruction of this framework is caused by the pyrolysis of organic molecules at high temperatures. Here, the bonds less stable than the M–N coordination ones are broken. The activation energies of this process are lower than those of the removal of the linker ligand, and accordingly, pre-exponential factors are very small.

The ratio between the kinetic parameters of these decomposition processes is such that an increase in the kinetic (thermal) stability of this framework can be related to steric hindrances and to the entropic factor rather than the enthalpic one.

Acknowledgements The authors are grateful to Netzsch Geratebau GmbH for the possibility of working with the computer program “NETZSCH Thermokinetics 2” and RFBR for financial support (Grant 11-03-00112-a).

References

- Zielenkiewicz W, Kozbiał M, Golankiewicz B, Poznanski J. Enhancement of aqueous solubility of tricyclic acyclovir derivatives by their complexation with hydroxypropyl- β -cyclodextrin. *J Therm Anal Calorim.* 2010;101:555–60.
- Zielenkiewicz W, Terekhova IV, Kozbiał M, Kumeev RS. Thermodynamic study on inclusion complex formation of

- riboflavin with hydroxypropyl- β -cyclodextrin in water. *J Therm Anal Calorim.* 2010;101:595–600.
3. Serafini MR, Menezes PP, Costa LP, Lima CM, Quintans LJ Jr, Cardoso JC, Matos JR, Soares-Sobrinho JL, Grangeiro S Jr, Nunes PS, Bonjadim LR, Araujo AAS. Interaction of *p*-cymene with β -cyclodextrin. *J Therm Anal Calorim.* 2011. doi:10.1007/s10973-011-1736-x.
 4. Dybtsev DN, Yutkin MP, Peresyphkina EV, Virovets AV, Serre C, Ferey G, Fedin VP. Isoreticular homochiral porous metal–organic structures with tunable pore sizes. *Inorg Chem.* 2007;46:6843–5.
 5. Dybtsev DN, Yutkin MP, Samsonenko DG, Fedin VP, Nuzhdin AL, Bezrukov AA, Bryliakov KP, Talsi EP, Belosludov RV, Mizuseki H, Kawazoe Y, Subbotin OS, Belosludov VR. Modular homochiral porous coordination polymers: rational design, enantioselective guest exchange sorption and ab initio calculations of host–guest interactions. *Chem Eur J.* 2010;10:348–56.
 6. Netzsch Thermokinetics. <http://www.netzsch-thermal-analysis.com/us/thermokinetics-workshop>.
 7. Kissinger HE. Reaction kinetics in differential thermal analysis. *Anal Chem.* 1957;29:1702–6.
 8. Friedman HL. Kinetics of thermal degradation of char-forming plastics from thermogravimetry. *J Polym Sci.* 1963;6:183–95.
 9. Ozawa T. A new method of analyzing thermogravimetric data. *Bull Chem Soc Japan.* 1965;38:1881–6.
 10. Ozawa T. Estimation of activation energy by isoconversion methods. *Thermochim Acta.* 1992;203:159–65.
 11. Flynn JH, Wall LA. General treatment of the thermogravimetry of polymers. *J Res Nat Bur Stand.* 1966;70:478–523.
 12. Opfermann J, Kaisersberger E. An advantageous variant of the Ozawa–Flynn–Wall analysis. *Thermochim Acta.* 1992;203:167–75.
 13. Opfermann JR, Kaisersberger E, Flammersheim HJ. Model-free analysis of thermo-analytical data—advantages and limitations. *Thermochim Acta.* 2002;391:119–27.
 14. Vyazovkin S. Model-free kinetics: staying free of multiplying entities without necessity. *J Therm Anal Calorim.* 2006;83:45–51.
 15. Simon P. Single-step kinetics approximation employing nonarrhenius temperature functions. *J Therm Anal Calorim.* 2005;79:703–8.
 16. Simon P. The single-step approximation: attributes, strong and weak sides. *J Therm Anal Calorim.* 2007;88:709–15.
 17. Vyazovkin S, Burnham AK, Criado JM, Luis A, Perez-Maqueda LA, Popescu C, Sbirrazzuoli N. ICTAC Kinetics Committee recommendations for performing kinetic computations on thermal analysis data. *Thermochim Acta.* 2011;520:1–19.
 18. Logvinenko V. Stability and reactivity of coordination and inclusion compounds in the reversible processes of thermal dissociation. *Thermochim Acta.* 1999;340(1):293–9.
 19. Logvinenko V. Solid state coordination chemistry. The quantitative thermoanalytical study of thermal dissociation reactions. *J Therm Anal Calorim.* 2000;60:9–15.
 20. Logvinenko V. Stability of supramolecular compounds under heating. Thermodynamic and kinetic aspects. *J Therm Anal Calorim.* 2010;101:577–83.
 21. Logvinenko V, Dybtsev D, Fedin V, Drebushchak V, Yutkin M. The stability of inclusion compounds under heating Part 2 Inclusion compounds of layered zinc camphorate, linked by linear N-donor ligands. *J Therm Anal Calorim.* 2010;100:183–9.